Determination of aqueous acid-dissociation constants of aspartic acid using PCM/DFT method

ARTICLE *in* INTERNATIONAL JOURNAL OF QUANTUM CHEMISTRY · DECEMBER 2007

Impact Factor: 1.43 · DOI: 10.1002/qua.21569

2 AUTHORS:

Wichien sang-aroon
Rajamangala University of Technology Isan
17 PUBLICATIONS **112** CITATIONS
SEE PROFILE

Vithaya Ruangpornvisuti
Chulalongkorn University
110 PUBLICATIONS **838** CITATIONS
SEE PROFILE

Determination of Aqueous Acid-Dissociation Constants of Aspartic Acid Using PCM/DFT Method

WICHIEN SANG-AROON, VITHAYA RUANGPORNVISUTI

Supramolecular Chemistry Research Unit, Department of Chemistry, Faculty of Science, Chulalongkorn University, Bangkok 10330, Thailand

Received 7 September 2007; accepted 16 October 2007
Published online 10 December 2007 in Wiley InterScience (www.interscience.wiley.com)
DOI 10.1002/qua.21569

ABSTRACT: Determination of acid-dissociation constants, pK_a, of aspartic acid in aqueous solution, using density functional theory calculations combined with the conductor-like polarizable continuum model (CPCM) and with integral-equation-formalism polarizable continuum model (IEFPCM) based on the UAKS and UAHF radii, was carried out. The computed pK_a values derived from the CPCM and IEFPCM with UAKS cavity model of bare structures of the B3LYP/6-31+G(d,p)-optimized tetrahydrated structures of aspartic acid species are mostly close to the experimental pK_a values. © 2007 Wiley Periodicals, Inc. Int J Quantum Chem 108: 1181–1188, 2008

Key words: aspartic acid; zwitterionic species; acid dissociation constant; DFT; CPCM; IEFPCM; solvent effect

Introduction

In equilibria of cationic, zwitterionic, and anionic species of aspartic acid were determined within the wide pH range of acidic to basic aqueous solutions [1, 2]. Dianionic species of aspartic acid (asp^{2-}) found in the aqueous solution at high pH range was introduced and its reaction rates are reported [2–4]. At the wide pH range of aqueous aspartic acid solution, the structures of species H_3asp^+, H_2asp, $Hasp^-$, and asp^{2-} have been mentioned [1–3, 5–8] as shown in Scheme 1. The potential energy surfaces of various species of aspartic acid have been computed at the DFT/B3LYP/6-31G(d) level of theory, and the most stable structures of species H_3asp^+, H_2asp, $Hasp^-$, and asp^{2-} are reported [7, 9]. The experimental acid-dissociation constants pK_{a1} = 2.10, pK_{a2} = 3.86, and pK_{a3} = 9.82 [8] obtained by the potentiometric titration method, pK_{a1} = 2.0, pK_{a2} = 3.9, and pK_{a3} = 9.8 [10]

Correspondence to: V. Ruangpornvisuti; e-mail: vithaya.r@chula.ac.th

Contract grant sponsor: Thailand Research Fund (TRF).
Contract grant sponsor: The Royal Golden Jubilee (RGJ) Grant.
Contract grant number: PHD46K0087.
This article contains supplementary material available via the Internet at http://www.interscience.wiley.com/jpages/0020-7608/suppmat.

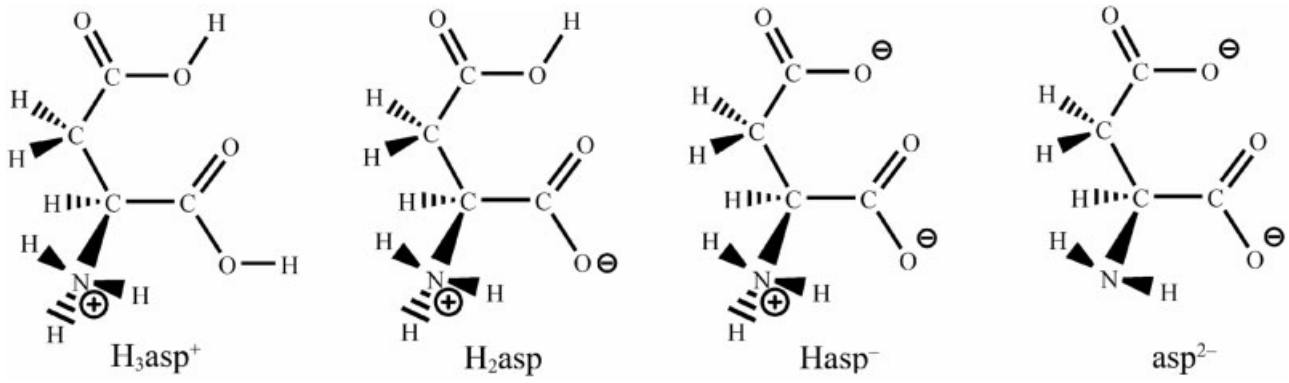

SCHEME 1.

by NMR titration method and pK_{a1} = 2.0, pK_{a2} = 3.9, and pK_{a3} = 10.0 [11] are reported.

In this work, we have studied acid dissociation of aspartic acid in aqueous solution using the density functional theory (DFT) calculations with two different solvation models, conductor-like polarizable continuum model (CPCM) and integral-equation-formalism polarizable continuum model (IEFPCM) based on two different cavity models, united-atom Kohn–Sham topological model (UAKS) and united atom for Hartree–Fock (UAHF). The acid-dissociation constants of aspartic acid derived from various solvation models in terms of pK_a values have been determined and compared to the experimental results. All results obtained from the solvation effect calculations have been reported.

Computational Details

QUANTUM CHEMICAL AND PCM SOLVATION MODELS

Structure optimizations of all species of aspartic acid were carried out using DFT method. The calculations have been performed with hybrid density functional B3LYP, the Becke's three-parameter exchange functional [12], and the Lee–Yang–Parr correlation functional [13] using 6-31+G(d,p) basis function. The structure optimizations of bare molecular structures of species H_3asp^+, H_2asp, $Hasp^-$, and asp^{2-} and their n-hydrated ($(H_2O)_n$, n = 3–6) structures have been carried out at the B3LYP/6-31+G(d,p) level of theory. The single-point calculations at the same level of theory have been employed for solvent-effect computations using the polarizable continuum model (PCM) of Tomasi and coworkers [14–20]. The CPCM [21–23] and IEFPCM [14, 15, 24, 25] have been used in the single-point calculations for the PCM solvent effect. The molecular cavity models used in the PCM models are UAHF [18] and UAKS [26].

Gibbs free energies (G_{gas}) of various species of aspartic acid in gas phase were obtained from the frequency calculations of the B3LYP/6-31+G(d,p). The solvation free energies (ΔG_{solv}) of the various species of aspartic acid in aqueous solution were obtained from the single-point B3LYP/6-31+G(d,p) calculations combined with the PCM models CPCM and IEFPCM with dielectric constant ε = 78.37 and using with the cavity models UAKS and UAHF.

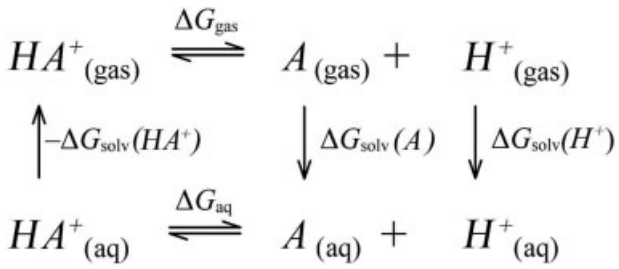

SCHEME 2.

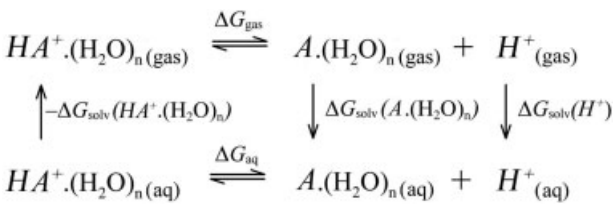

SCHEME 3.

All calculations were performed with the Gaussian 03 program [26]. The GaussView 3.07 program [27] was utilized to build molecular structures, display molecular geometry convergence, and generate molecular graphics of all related species.

THERMODYNAMIC CYCLES AND ACID-DISSOCIATION MODELS

Thermodynamic cycles for calculations of the theoretical pK_{a1}, pK_{a2}, and pK_{a3} for acid dissociations of aspartic acid species Hasp, H_2asp^+, and asp^- are shown in the Scheme 2 as representative for the bare structure system and in the Scheme 3 as representative of the *n*-hydrated system, respectively. These thermodynamic cycles are modified from the cycles which are taken from Refs. 28 and 29. The first (pK_{a1}), second (pK_{a2}), and third (pK_{a3}) dissociation constants are defined using the well-known thermodynamic Eq. (1).

$$pK_a = \Delta G_{aq}/2.303RT \quad (1)$$

The Gibbs free energies of aqueous acid-dissociation reactions are computed by adding a solvation contribution to the gas phase value using the following equations.

$$\Delta G_{aq} = \Delta G_{gas} + \Delta\Delta G_{solv} \quad (2)$$

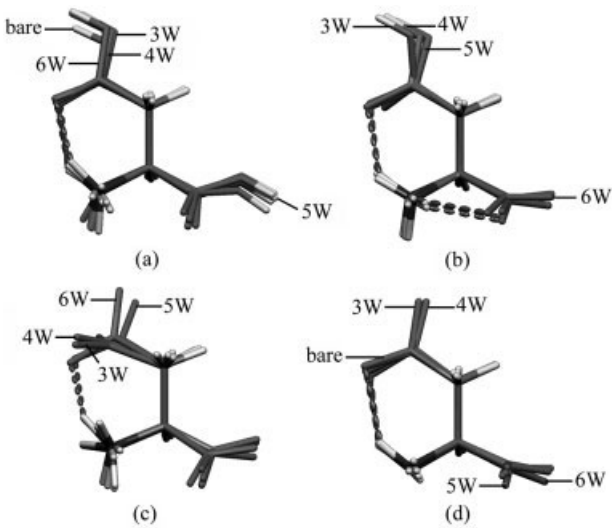

FIGURE 1. Superimposition of the B3LYP/6-31+G(d,p)-optimized structures of various states of the most stable species of L-aspartic acid as forms: (a) H_3asp^+, (b) H_2asp, (c) $Hasp^-$, and (d) asp^{2-}. For clarity, water molecules are not shown.

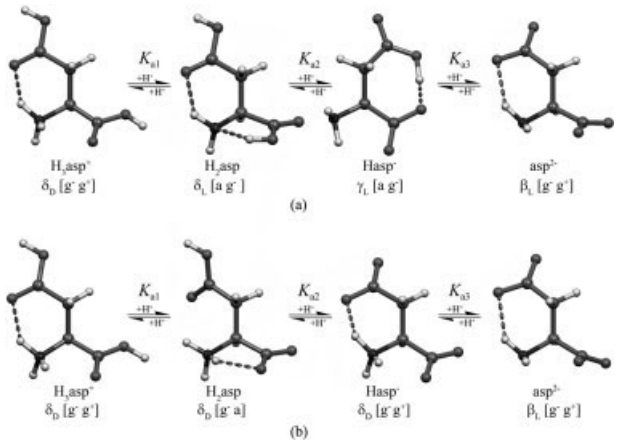

FIGURE 2. The acid-dissociation equilibria of aspartic acid in gas phase presented as (a) the bare structures and (b) hexahydrated species. For clarity, the six water molecules for hexahydrated species are not shown and the Ramachandran/IUPAC nomenclatures for conformations of aspartic acid species are given at the bottom of each molecule.

$$\Delta G_{gas} = G_{gas}(A) + G_{gas}(H^+) - G_{gas}(AH^+) \quad (3)$$

$$\Delta\Delta G_{solv} = \Delta G_{solv}(A) + \Delta G_{solv}(H^+) - \Delta G_{solv}(HA^+) \quad (4)$$

where AH^+ and A are species for AH^+ to A dissociation as representative for dissociations of H_3asp to H_2asp, H_2asp to $Hasp^-$ and $Hasp^-$ to asp^{2-}. Thermodynamic cycles for calculations of the theoretical pK_{a1}, pK_{a2}, and pK_{a3} for acid dissociations of aspartic acid species H_3asp^+, H_2asp, and $Hasp^-$ are shown in Schemes S-1, S-2, and S-3 for their bare structures and Schemes S-4, S-5, and S-6 for their *n*-hydrated, $n = 3–6$, structures, respectively. The entire equations of Gibbs free energies for dissociations of H_3asp^+ to H_2asp, H_2asp to $Hasp^-$ and $Hasp^-$ to asp^{2-} are shown in Eqs. (S-1)–(S-3), (S-4)–(S-6) and (S-7)–(S-9), respectively. As experimental derivation, $\Delta G_{gas}(H^+) = -6.28$ kcal/mol (at the reference state of 1 atm)[30] and $\Delta G_{solv}(H^+) = -264.61$ kcal/mol (at the reference state of 1 M)[31] were used in the calculations.

Results and Discussion

The B3LYP/6-31+G(d,p)-optimized geometries of bare and *n*-hydrated ($(H_2O)_n$, $n = 3–6$) structures of aspartic acid species H_3asp^+, H_2asp, $Hasp^-$, and

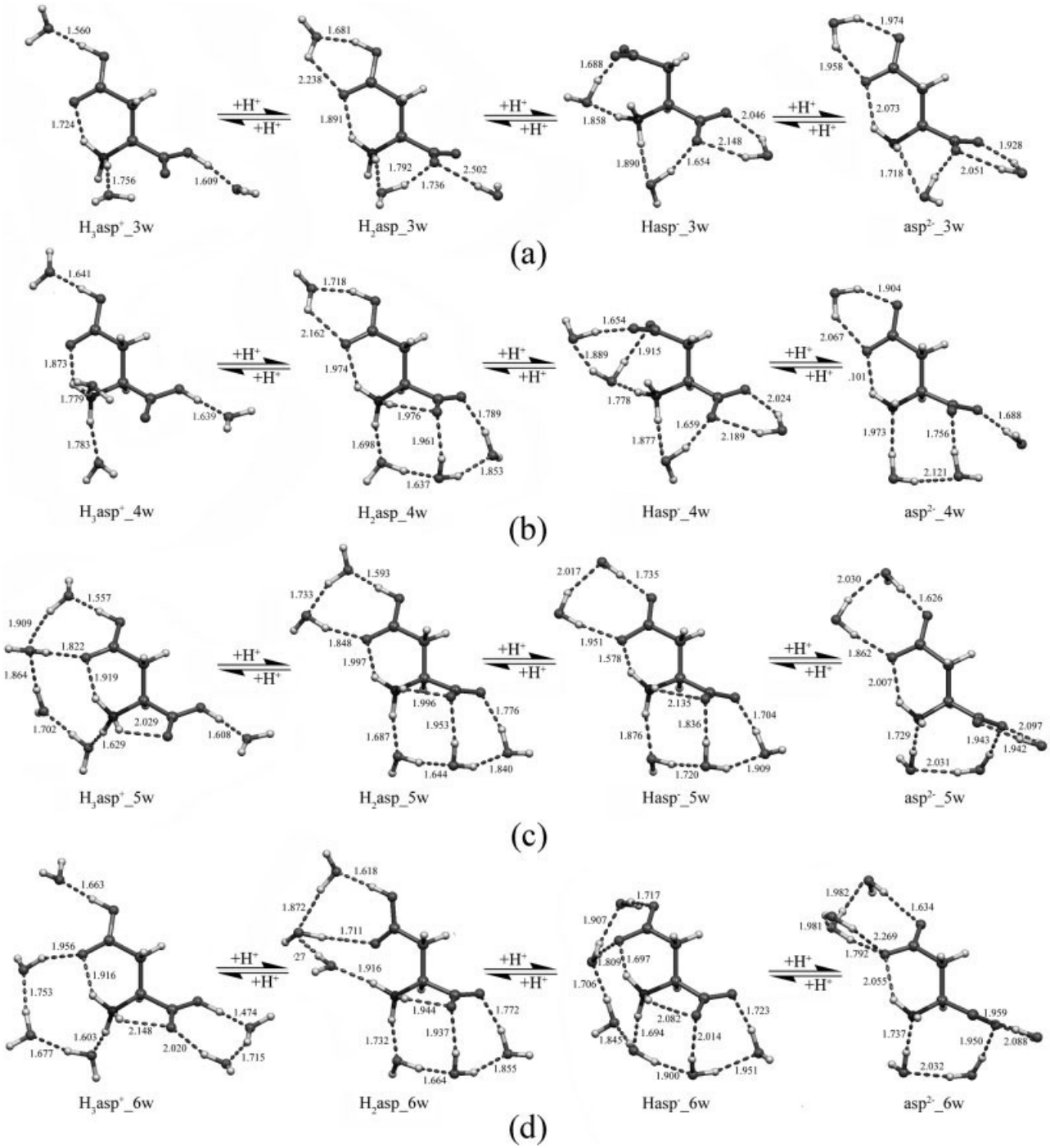

FIGURE 3. The acid-dissociation equilibria of aspartic acid based on their (a) tri-, (b) tetra-, (c) penta-, and (d) hexahydrated structures. The hydrogen bond distances are in Angstroms.

asp^{2-} were obtained and their superimposed structures are shown in Figure 1. The bare structures for species H_2asp and $Hasp^-$ are not included in Figure 1, because their gas-phase structures are in the conformations $\delta_L[a\ g^-]$ and $\gamma_L[a\ g^-]$ which are different from their aqueous-phase structures. The acid-dissociation equilibria of aspartic acid species in gas phase as the bare and hexahydrated structures are

shown in Figure 2. It shows the conformations defined by Ramachandran nomenclature [7, 32] and IUPAC nomenclature [33] of aspartic acid species in gas phase and aqueous system which is represented by hexahydrated system. Conformations of aspartic acid species H_3asp^+, H_2asp, $Hasp^-$, and asp^{2-} in forms of hexahydrated forms are $\delta_D[g^- g^+]$, $\delta_D[g^- a]$, $\delta_D[g^- g^+]$ and $\beta_L[g^- g^+]$, respectively.

The conformations of free structures of aspartic acid species H_3asp^+ and asp^{2-} are the same conformations of their corresponding species of *n*-hydrated (n = 3–6) structures. The conformations of free forms of aspartic acid species H_2asp ($\delta_L[a\ g^-]$) and $Hasp^-$ ($\gamma_L[a\ g^-\ ]$) are different from their *n*-hydrated (n = 3–6) structures. All the *n*-hydrated structures of various species of aspartic acid and their equilibria are shown in Figure 3. The computed pK_a values and Gibbs free energy contributions for acid-dissociation equilibria of free-form bare structures, bare structures of *n*-hydrated forms, and *n*-hydrated forms of aspartic acid species are listed in Tables I–III, respectively.

Based on the bare structural system, the cavity models (UAKS and UAHF) cause different pK_a values, rather than the PCM (CPCM and IEFPCM) models and the PCM/UAHF model's result, and the predicted pK_a values are very close to the experimental results, as shown in Table I.

The correlation coefficients (r^2) of the computed and measured pK_a values of aspartic acid species are shown in Table S-I, supplementary material. As the high correlations of the computed pK_a values for the bare structures of free form system with the experimental values taken from Ref. 8 were considered, the small different pK_a values, $\Delta pK_{a1} = -0.17$ (1.93–2.10), $\Delta pK_{a2} = 0.24$ (4.10–3.86), and $\Delta pK_{a3} = -0.07$ (9.75–9.82) with $r^2 = 0.9972$ for CPCM/UAHF model and $\Delta pK_{a1} = -0.18$ (1.92–2.10), $\Delta pK_{a2} = 0.25$ (4.11–3.86), and $\Delta pK_{a3} = -0.07$ (9.75–9.82) with $r^2 = 0.9970$ for IEFPCM/UAHF model were obtained. Based on the equilibrium system for bare structures of *n*-hydrated forms of aspartic acid species, computed pK_a values for tri- and tetrahydrated systems are mostly close to the experimental values.

The different pK_a values for the bare structures of aspartic acid species of trihydrated system, $\Delta pK_{a1} = 0.09$ (2.19–2.10), $\Delta pK_{a2} = -0.14$ (3.72–3.86), and $\Delta pK_{a3} = 0.01$ (9.83–9.82) with $r^2 = 0.9992$ for CPCM/UAKS model and $\Delta pK_{a1} = -0.12$ (1.98–2.10), $\Delta pK_{a2} = 0.16$ (4.02–3.86), and $\Delta pK_{a3} = -0.04$ (9.78–9.82) with $r^2 = 0.9987$ for IEFPCM/UAKS

TABLE I

Gibbs free energy contributions ΔG_{gas}, $\Delta\Delta G_{solv}$, and ΔG_{aq} (kcal/mol) for the acid-dissociation equilibria of bare structures of aspartic acid species, computed at the B3LYP/6-31+G(d,p) level.

		CPCM		IEFPCM		pK_a		
Deprotonation	ΔG_{gas}	$\Delta\Delta G_{solv}$ [a]	ΔG_{aq} [b]	$\Delta\Delta G_{solv}$ [a]	ΔG_{aq} [b]	Calc.[c]	Calc.[d]	Exp.[e]
$H_3asp^+ \rightarrow H_2asp + H^+$	211.82	−208.66 (−208.83)	3.16 (2.99)	−208.66 (−208.83)	3.16 (2.99)	1.93 (1.42)	1.92 (1.42)	2.10
$H_2asp \rightarrow Hasp^- + H^+$	311.24	−304.49 (−304.10)	6.75 (7.14)	−304.49 (−304.10)	6.75 (7.14)	4.10 (5.18)	4.11 (5.19)	3.86
$Hasp^- \rightarrow asp^{2-} + H^+$	415.95	−399.91 (−404.42)	16.04 (11.53)	−399.91 (−404.42)	16.04 (11.53)	9.75 (9.18)	9.75 (9.17)	9.82

[a] The $\Delta\Delta G_{solv}$ values were obtained from single-point calculations at the B3LYP/6-31+G(d,p) level with UAKS and UAHF (in parentheses) cavity models.
[b] The ΔG_{aq} values were computed according to the thermodynamic cycles as shown in Schemes S-1, S-2, and S-3.
[c] Because of the CPCM with UAKS and UAHF (in parentheses) cavity models.
[d] Because of the IEFPCM with UAKS and UAHF (in parentheses) cavity models.
[e] Taken from Ref. 8.

TABLE II

Gibbs free energy contributions ΔG_{gas}, $\Delta\Delta G_{solv}$, and ΔG_{aq} (kcal/mol) for the acid-dissociation equilibria of bare structures of the B3LYP/6-31+G(d,p)-optimized *n*-hydrated forms of aspartic acid species in gas phase and aqueous solutions.

Hydrated system/reaction	ΔG_{gas}	CPCM			IEFPCM		
		$\Delta\Delta G_{solv}$[a]	ΔG_{aq}[b]	pK_a[c]	$\Delta\Delta G_{solv}$[a]	ΔG_{aq}[b]	pK_a[d]
Trihydrated							
$H_3asp^+ \rightarrow H_2asp + H^+$	233.23	−235.44 (−233.29)	−2.21 (−0.06)	1.74 (2.19)	−233.29 (−235.44)	−0.06 (−2.21)	1.67 (1.98)
$H_2asp \rightarrow Hasp^- + H^+$	314.74	−311.12 (−307.89)	3.62 (6.85)	4.18 (3.72)	−307.89 (−311.12)	6.85 (3.62)	4.54 (4.02)
$Hasp^- \rightarrow asp^{2-} + H^+$	390.34	−370.29 (−371.37)	20.05 (18.97)	9.24 (9.83)	−371.37 (−370.29)	18.97 (20.05)	9.57 (9.78)
Tetrahydrated							
$H_3asp^+ \rightarrow H_2asp + H^+$	228.29	−230.11 (−228.02)	−1.82 (0.27)	1.83 (2.17)	−228.02 (−230.11)	0.27 (−1.82)	1.84 (2.17)
$H_2asp \rightarrow Hasp^- + H^+$	320.63	−317.62 (−314.28)	3.01 (6.35)	4.21 (3.75)	−314.28 (−317.62)	6.35 (3.01)	4.21 (3.77)
$Hasp^- \rightarrow asp^{2-} + H^+$	389.62	−368.25 (−369.44)	21.37 (20.18)	9.69 (9.83)	−369.44 (−368.25)	20.18 (21.37)	9.61 (9.84)
Pentahydrated							
$H_3asp^+ \rightarrow H_2asp + H^+$	226.79	−231.75 (−229.50)	−4.96 (−2.71)	2.52 (2.67)	−229.50 (−231.75)	−2.71 (−4.96)	2.52 (2.67)
$H_2asp \rightarrow Hasp^- + H^+$	304.43	−306.82 (−303.69)	−2.39 (0.74)	3.38 (3.24)	−303.69 (−306.82)	0.74 (−2.39)	3.38 (3.24)
$Hasp^- \rightarrow asp^{2-} + H^+$	404.42	−376.35 (−377.54)	28.07 (26.88)	9.87 (9.87)	−377.54 (−376.35)	26.88 (28.07)	9.88 (9.87)
Hexahydrated							
$H_3asp^+ \rightarrow H_2asp + H^+$	229.46	−233.79 (−231.44)	−4.33 (−1.98)	2.65 (2.78)	−231.44 (−233.79)	−1.98 (−4.33)	2.66 (2.78)
$H_2asp \rightarrow Hasp^- + H^+$	304.19	−306.88 (−303.79)	−2.69 (0.40)	3.26 (3.14)	−303.79 (−306.88)	0.40 (−2.69)	3.25 (3.14)
$Hasp^- \rightarrow asp^{2-} + H^+$	402.13	−373.73 (−375.09)	28.40 (27.04)	9.87 (9.86)	−375.09 (−373.73)	27.04 (28.40)	9.87 (9.86)

[a] The $\Delta\Delta G_{solv}$ values were obtained from single-point calculation at the B3LYP/6-31+G(d,p) level with UAKS and UAHF (in parentheses) cavity models.
[b] The ΔG_{aq} values were computed according to the thermodynamic cycles as shown in Schemes S-1, S-2, and S-3.
[c] Because of the CPCM with UAKS and UAHF (in parentheses) cavity models.
[d] Because of the IEFPCM with UAKS and UAHF (in parentheses) cavity models.

TABLE III

Gibbs free energy contributions ΔG_{gas}, $\Delta\Delta G_{solv}$, and ΔG_{aq} (kcal/mol) for the acid-dissociation equilibria of the B3LYP/6-31+G(d,p)-optimized *n*-hydrated structures of aspartic acid species in gas phase and aqueous solutions.

Hydrated model/reaction	ΔG_{gas}	CPCM			IEFPCM		
		$\Delta\Delta G_{solv}$[a]	ΔG_{aq}[b]	pK_a[c]	$\Delta\Delta G_{solv}$[a]	ΔG_{aq}[b]	pK_a[d]
Trihydrated							
$H_3asp^+.(H_2O)_3 \rightarrow H_2asp.(H_2O)_3 + H^+$	248.70	−234.92 (−235.63)	13.78 (13.07)	6.02 (7.84)	−234.93 (−235.65)	13.77 (13.05)	6.04 (4.75)
$H_2asp.(H_2O)_3 \rightarrow Hasp^-.(H_2O)_3 + H^+$	303.33	−294.93 (−297.54)	8.40 (5.79)	7.44 (2.50)	−294.91 (−297.50)	8.42 (5.83)	7.41 (6.51)
$Hasp^-.(H_2O)_3 \rightarrow asp^{2-}.(H_2O)_3 + H^+$	381.32	−361.33 (−360.60)	19.99 (20.72)	12.22 (13.44)	−361.56 (−360.70)	19.76 (20.62)	12.06 (12.46)
Tetrahydrated							
$H_3asp^+.(H_2O)_4 \rightarrow H_2asp.(H_2O)_4 + H^+$	243.60	−231.02 (−232.76)	12.58 (10.84)	6.79 (6.20)	−231.00 (−232.74)	12.60 (10.86)	6.80 (5.26)
$H_2asp.(H_2O)_4 \rightarrow Hasp^-.(H_2O)_4 + H^+$	309.18	−297.42 (−299.51)	11.76 (9.67)	7.76 (5.34)	−297.44 (−299.51)	11.74 (9.67)	7.75 (6.58)
$Hasp^-.(H_2O)_4 \rightarrow asp^{2-}.(H_2O)_4 + H^+$	375.83	−358.08 (−357.90)	17.75 (17.93)	11.06 (11.40)	−358.20 (−358.03)	17.63 (17.80)	10.98 (11.02)
Pentahydrated							
$H_3asp^+.(H_2O)_5 \rightarrow H_2asp.(H_2O)_5 + H^+$	240.14	−234.62 (−235.71)	5.52 (4.97)	1.16 (1.90)	−234.59 (−235.14)	5.55 (5.00)	1.17 (0.27)
$H_2asp.(H_2O)_5 \rightarrow Hasp^-.(H_2O)_5 + H^+$	303.15	−296.85 (−298.69)	6.30 (4.46)	4.36 (1.53)	−296.86 (−298.67)	6.29 (4.48)	4.36 (3.69)
$Hasp^-.(H_2O)_5 \rightarrow asp^{2-}.(H_2O)_5 + H^+$	377.74	−354.14 (−353.77)	23.60 (23.97)	15.22 (15.83)	−354.23 (−353.87)	23.51 (23.87)	15.15 (15.26)
Hexahydrated							
$H_3asp^+.(H_2O)_6 \rightarrow H_2asp.(H_2O)_6 + H^+$	243.05	−234.36 (−235.22)	8.69 (7.83)	3.02 (3.99)	−234.37 (−235.24)	8.68 (7.81)	3.03 (1.74)
$H_2asp.(H_2O)_6 \rightarrow Hasp^-.(H_2O)_6 + H^+$	301.60	−294.15 (−296.55)	7.45 (5.05)	5.79 (1.96)	−294.12 (−296.50)	7.48 (5.10)	5.79 (4.89)
$Hasp^-.(H_2O)_6 \rightarrow asp^{2-}.(H_2O)_6 + H^+$	374.44	−350.71 (−349.79)	23.73 (24.65)	15.17 (16.32)	−350.81 (−349.91)	23.63 (24.53)	15.11 (15.57)

[a] The $\Delta\Delta G_{solv}$ values were obtained from single-point calculations at the B3LYP/6-31+G(d,p) level with UAKS and UAHF (in parentheses) cavity models.
[b] The ΔG_{aq} values were computed according to the thermodynamic cycles as shown in Schemes S-4, S-5, and S-6.
[c] Because of the CPCM with UAKS and UAHF (in parentheses) cavity models.
[d] Because of the IEFPCM with UAKS and UAHF (in parentheses) cavity models.

model were obtained as the second most accurate values. The most accurate prediction due to the bare structures of aspartic acid species of tetrahydrated system was found with different pK_a values: $\Delta pK_{a1} = 0.07$ (2.17–2.10), $\Delta pK_{a2} = -0.11$ (3.75–3.86), and $\Delta pK_{a3} = 0.01$ (9.83–9.82) with $r^2 = 0.9995$ for CPCM/UAKS model and $\Delta pK_{a1} = 0.07$ (2.17–2.10), $\Delta pK_{a2} = -0.09$ (3.77–3.86), and $\Delta pK_{a3} = 0.02$ (9.84–9.82) with $r^2 = 0.9996$ for IEFPCM/UAKS model were obtained.

Complete sets of the computed pK_a values for *n*-hydrated systems (Table III) are really different from the experimental results. This must be the limitation of these two cavity models of solvent-effect calculation on the water-added system. Deviation of the pK_a values of complete sets for the *n*-hydrated structures of aspartic acid species from their experimental values corresponds to the previously inaccurate results of solvent-effect calculations for the trihydrated system of 5-hydroxytryptamine, as reported in Ref. 29. Nevertheless, thermodynamic quantities of hydration reaction of aspartic acid species of *n*-hydrated models are shown in Table S-II.

Conclusions

Acid-dissociation constants of aspartic acid in aqueous solution were determined using the DFT, with two different solvation models of CPCM and IEFPCM based on two different cavity models of UAKS and UAHF. We found that the pK_a values derived from the CPCM and IEFPCM with UAKS cavity model of the bare B3LYP/6-31+G(d,p)-optimized structures of tetrahydrated aspartic acid species are mostly close to the experimental pK_a values. These two different solvation models of CPCM and IEFPCM are excellent methods for determination of acid-dissociation constants of the system of bare structures of aspartic acid as the conformations of $\delta_D[g^- g^+]$ for H_3asp^+, $\delta_D[g^- a]$ for H_2asp, $\delta_D[g^- g^+]$ for $Hasp^-$, and $\beta_L[g^- g^+]$ for asp^{2-} species.

References

1. Edsall, J. T.; Blanchard, M. H. J Am Chem Soc 1933, 55, 2337.
2. Noszál, B.; Sándor, P. Phys Chem 1986, 90, 6345.
3. Noszál, B.; Sándor, P. Anal Chem 1989, 61, 2631.
4. Sang-aroon, W.; Ruangpornvisuti, V. J Mol Graph Model 2007, 26, 342.
5. Smith, P. K.; Smith, E. R. B. J Biol Chem 1942, 146, 187.
6. West, R. C. CRC Handbook of Chemistry and Physics, 66th ed., CRC Press: Boca Raton, FL, 1985.
7. Sang-aroon, W.; Ruangpornvisuti, V. J Mol Struct (THEOCHEM) 2006, 758, 181.
8. Ruangpornvisuti, V.; Tomapatanaget, B. SciAsia 2003, 29, 45.
9. Sang-aroon, W.; Ruangpornvisuti, V. J Mol Struct (THEOCHEM) 2006, 765, 153.
10. Tananaeva, N. N.; Gorokhovatskaya, M. Y.; Tikhonova, R. V.; Kostromina, N. A. Theor Exp Chem 1985, 21, 471.
11. Mahler, R. H.; Eugen, H. C. Biological Chemistry, 2nd ed.; Harper and Row Publishers: New York, 1971.
12. Becke, A. D. J Chem Phys 1993, 98, 5648.
13. Lee, C.; Yang, W.; Parr, R. G. Phys Rev B 1988, 37, 785.
14. Cancès, M. T.; Mennucci, B.; Tomasi, J. J Chem Phys 1997, 107, 3032.
15. Mennucci, B.; Tomasi, J. J Chem Phys 1997, 106, 5151.
16. Cossi, M.; Barone, V.; Mennucci, B.; Tomasi, J. Chem Phys Lett 1998, 286, 253.
17. Barone, V.; Cossi, M.; Tomasi, J. J Comput Chem 1998, 19, 404.
18. Barone, V.; Cossi, M.; Tomasi, J. J Chem Phys 1997, 107, 3210.
19. Cossi, M.; Barone, V.; Cammi, R.; Tomasi, J. Chem Phys Lett 1996, 255, 327.
20. Miertus, S.; Tomasi, J. Chem Phys 1982, 65, 239.
21. Cossi, M.; Rega, N.; Scalmani, G.; Barone, V. J Comput Chem 2003, 24, 669.
22. Cossi, M.; Barone, V. J Chem Phys 1998, 109, 6246.
23. Barone, V.; Cossi, M. J Phys Chem A 1995, 1998, 102.
24. Mennucci, B.; Cances, E.; Tomasi, J. J Phys Chem B 1997, 101, 10506.
25. Tomasi, J.; Mennucci, B.; Cances, E. J Mol Struct (THEOCHEM) 1999, 464, 211.
26. Frisch M. J.; Trucks, G. W.; Schlegel, H. B.; Scuseria, G. E.; Robb, M. A.; Cheeseman, J. R.; Montgomery, J. A., Jr.; Vreven, T.; Kudin, K. N.; Burant, J. C.; Millam, J. M.; Iyengar, S. S.; Tomasi, J.; Barone, V.; Mennucci, B.; Cossi, M.; Scalmani, G.; Rega, N.; Petersson, G. A.; Nakatsuji, H.; Hada, M.; Ehara, M.; Toyota, K.; Fukuda, R.; Hasegawa, J.; Ishida, M.; Nakajima, T.; Honda, Y.; Kitao, O.; Nakai, H.; Klene, M.; Li, X.; Knox, J. E.; Hratchian, H. P.; Cross, J. B.; Adamo, C.; Jaramillo, J.; Gomperts, R.; Stratmann, R. E.; Yazyev, O.; Austin, A. J.; Cammi, R.; Pomelli, C.; Ochterski, J. W.; Ayala, P. Y.; Morokuma, K.; Voth, G. A.; Salvador, P.; Dannenberg, J. J.; Zakrzewski, V. G.; Dapprich, S.; Daniels, A. D.; Strain, M. C.; Farkas, O.; Malick, D. K.; Rabuck, A. D.; Raghavachari, K.; Foresman, J. B.; Ortiz, J. V.; Cui, Q.; Baboul, A. G.; Clifford, S.; Cioslowski, J.; Stefanov, B. B.; Liu, G.; Liashenko, A.; Piskorz, P.; Komaromi, I.; Martin, R. L.; Fox, D. J.; Keith, T.; Al-Laham, M. A.; Peng, C. Y.; Nanayakkara, A.; Challacombe, M.; Gill, P. M. W.; Johnson, B.; Chen, W.; Wong, M. W.; Gonzalez, C.; Pople, J. A. Gaussian 03, Revision D02; Gaussian: Wallingford, CT, 2006.
27. Dennington II, R.; Keith, T.; Millam, J.; Eppinnett, K.; Hovell,

W. L.; Gilliland, R. GaussView, Version 3.07, Semichem, Inc.: Shawnee Mission, KS, 2003.

28. Kelly, C. P.; Cramer, C. J.; Truhlar, D. G. J Phys Chem A 2006, 110, 2493.
29. Pratuangdejkul, J.; Nosoongnoen, W.; Guérin, G.-A.; Loric, S.; Conti, M.; Launay, J.-M.; Manivet, P. Chem Phys Lett 2006, 420, 538.
30. Topol, I. A.; Tawa, G. J.; Burt, S. K.; Rashin, A. A. J Chem Phys 1999, 111, 10998.
31. Liptak, M. D.; Shields, G. C. J Am Chem Soc 2001, 123, 7314.
32. Chakrabarti, P.; Pal, D. Prog Biophys Mol Biol 2001, 76, 1.
33. Dordrecht, D. R. IUPAC-IUB commission on biochemical nomenclature. Biochemistry 1970, 9, 3471.